NATIONAL RADIO ASTRONOMY OBSERVATORY
Green Bank, West Virginia

Electronics Division Internal Report No. 103

MARK II THERMAL CALIBRATOR

J. W. Findlay and J. Payne

AUGUST 1971

MARK II THERMAL CALIBRATOR

TABLE OF CONTENTS

LIST OF FIGURES

MARK II THERMAL CALIBRATOR

J. W. Findlay and J. Payne

1.0   Introduction

The usual method of calibrating radiometers is to change the temperature of an RF load connected to the radiometer input. For the past four years we have been using a thermal calibrator consisting of a temperature-controlled RF load, the control element being thermoelectric heat pumps. A servo system keeps the load at the required temperature, the sensor being a thermistor and the readout device a mercury thermometer. This method is faster, more accurate, and considerably more convenient than the more traditional method of dunking a suitably encased load in water of various temperatures.

The Mark II Thermal Calibrator uses the same principles but is a little more refined. A platinum resistance thermometer with a bridge acts as the sensing element and together with a digital voltmeter also serves as a temperature monitor, the readout being displayed digitally in degrees Centigrade to an accuracy of 1/100 °C.

Work at the calibration horn involving measurements on Cas A has resulted in an accurate comparison between the Mark I and Mark II thermal calibrators. At 1400 MHz the noise outputs from the two units for a given temperature swing agree to within one percent.

2.0   Description of Mark II Calibrator

2.1   Mechanical Details

Figure 1 is a photograph of the calibrator. Two temperatures, hot and cold, may be set on two dials, hot or cold, being selected by a switch. An "auto" position is available which causes automatic cycling between the two states every 4 minutes. The load temperature is displayed digitally in °C and may be set to any value between 10 °C and 50 °C.

The mechanical construction of the RF head is shown in Figure 2. Five thermoelectric heat pumps change the temperature of an aluminum block containing the RF load. The platinum sensor is placed very close to the load to minimize the effect of any temperature graduation across the aluminum block.
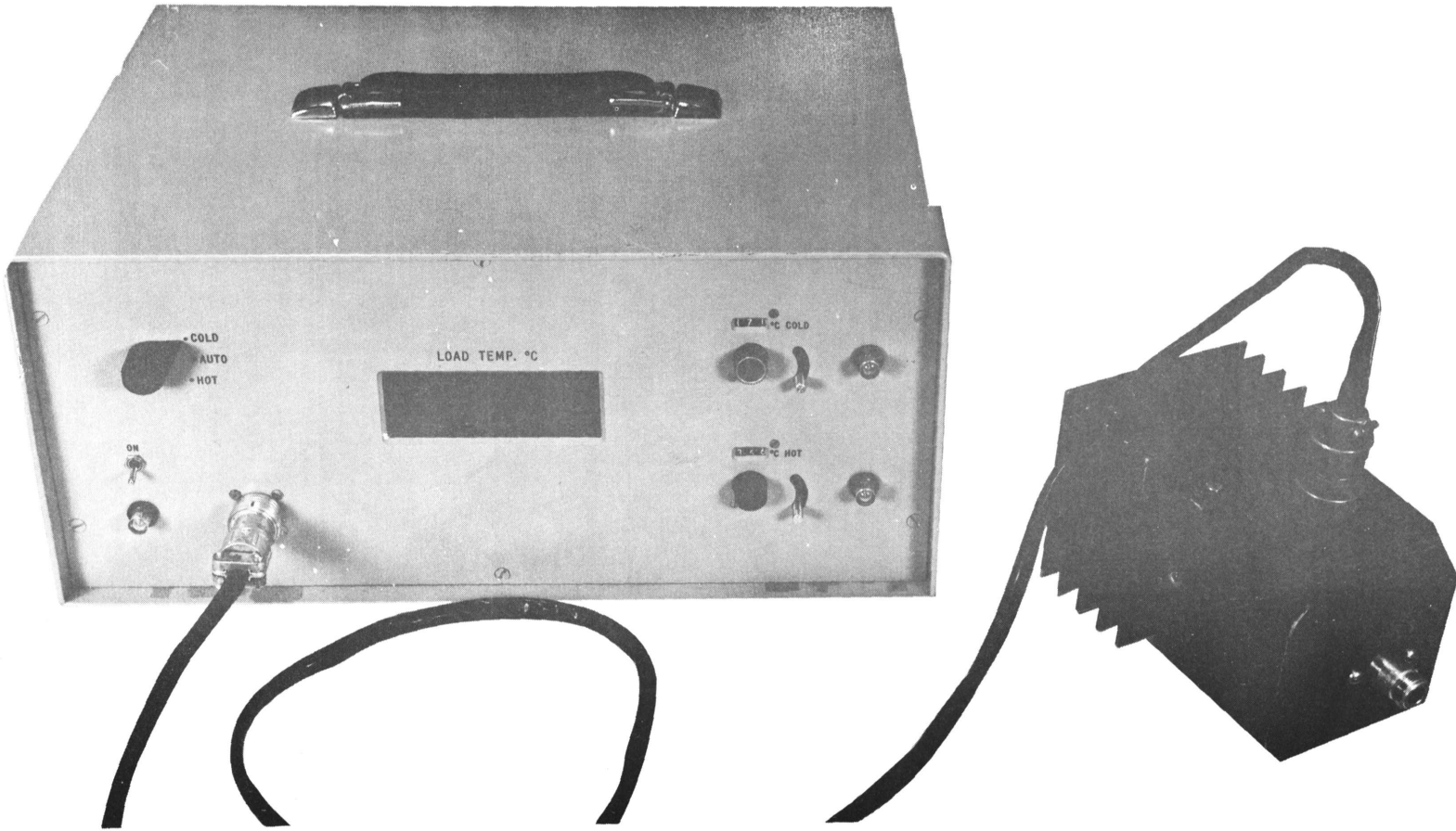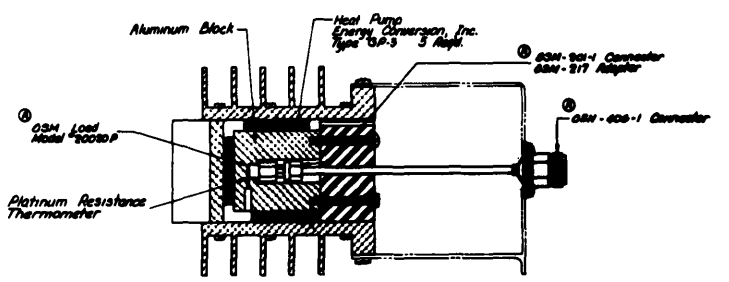
Figure 1 — Photograph of Calibrator

B↓

↓A   A↓

143-6P Amp.

Top View

Rear View   *Side View*   *Front View*

Aluminum Block

Heat Pump
Energy Conversion, Inc.
Type "GP-3" 3 Reqd.

OSM-351-1 Connector
OSM-217 Adapter

OSM Load
Model "200BD P"

OSM-206-1 Connector

Platinum Resistance
Thermometer
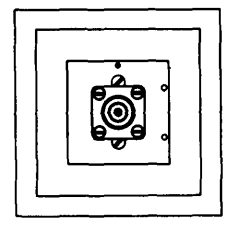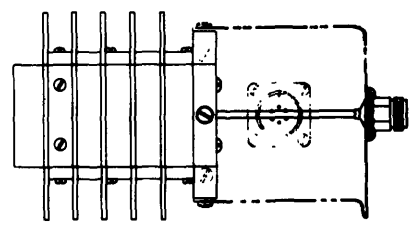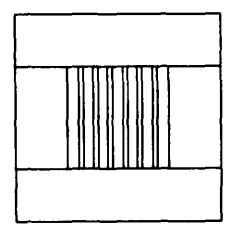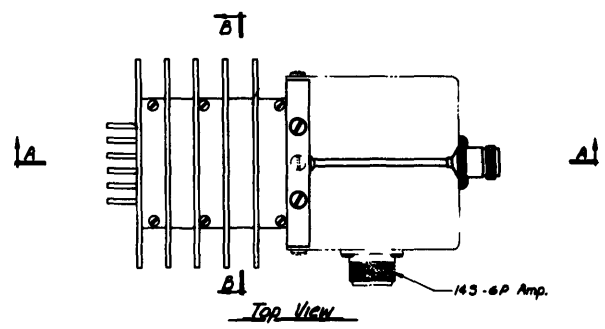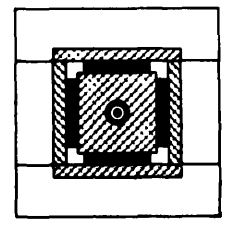
Section A-A   *Section B-B*

NATIONAL RADIO ASTRONOMY OBSERVATORY				
ASSOCIATED UNIVERSITIES INC.				
GREEN BANK, W. VA.				
R.F. HEAD for THERMAL CAL. UNIT				

SCALE Full	NO. 18 D 00009

2.2 Control Circuits (Figure 3)

The platinum sensor and associated bridge are manufactured by Rosemont Engineering. The bridge gives a voltage output that varies linearly with sensor temperature, the output in millivolts being equal to the sensor temperature in °C.

The output from the bridge is displayed on the front panel digital voltmeter. The bridge output is also used in the servo loop. After passing through a 60 Hz notch filter, the bridge output is amplified by A1. The temperature demand is generated by either the "hot" or "cold" potentiometer via A2 or A3. This voltage is subtracted from the output of A1, the difference being the error voltage.

The error voltage is then amplified by A4, phase shaped by the lag-lead network of A5 and further amplified by A6. The resultant voltage is then used to drive the power amplifier consisting of A7 and associated components which in turn drives the heat pumps.

When swinging between two temperatures we have found the repeatability to be around several hundreths of a degree.

3.0 Performance of the Mark II Thermal Calibrator

3.1 Introduction

Three important questions have to be considered in order to judge the accuracy of measurements made with a thermal noise source.

(a) Does the noise power available at the output port change by

$$\Delta P = kB\Delta T \qquad (1)$$

when the load temperature indicator shows a temperature change of ΔT°K?

(b) Is this change of available noise power completely transferred to the radiometer being calibrated?

(c) How rapidly does ΔP change when ΔT is altered? What time should be allowed for the source to stabilize in its noise output?

We will now summarize the information so far available on these three points.

3.2 The Available Noise Power

The design of the instrument is intended to ensure that the resistive element does in fact change in temperature by the amount shown on the indicator. This has been tested by comparing the instrument with other methods of calibrating radiometers. We have
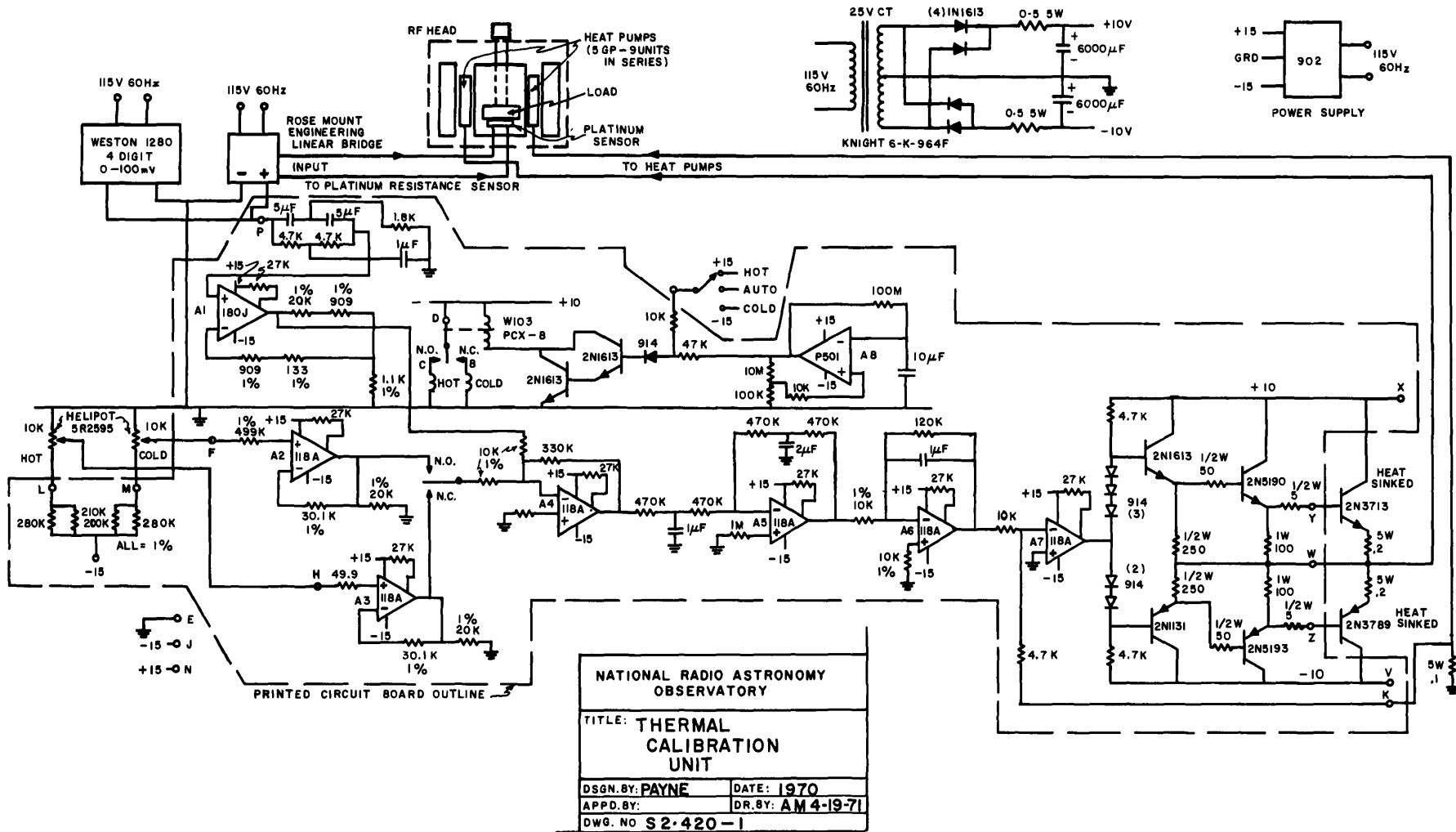
Figure 3 — Circuit Diagram

also estimated the losses in noise power due to the short length of line joining the load to its output port (the type N connector) and due to any other connectors or transitions used between the output port and the radiometer input.

3.21 The Effects of Line, Connector and Transition Losses

3.211 The loss in the line within JP 2

The line loss has been measured over the frequency range 1-11 GHz. The temperature gradient (when the load differs from room temperature) has also been measured. Corrections for these effects have been calculated, using the procedure of Stelzried (1968), and the results are summarized in the section on corrections (paragraph 3. 5).

3.212 Connector losses

The loss in the connection between the OSM line in JP 2 and its output Type N connector has also been measured over the 1-11 GHz range and its effect included in the corrections. The loss in the junction of the output port Type N to the radiometer input is <u>not</u> included, since a similar loss occurs when an antenna is joined to the radiometer input via a type N connector.

3.213 Transition losses

Although JP 2 is intended to be a coaxial noise source, it can be used with radiometers which use a waveguide input. To do this, the output port of JP 2 is connected via a coaxial-to-waveguide transition to the radiometer input. Losses in such transitions have been measured over the 1-11 GHz range and are allowed for in paragraph 3. 5.

3.22 Comparison with Other Thermal Sources

In the course of work with the calibration horn, a number of comparisons of thermal noise sources have been made. Measurements have usually been at or near 1400 MHz. The following table summarizes some of the more recent results.

In summary, therefore, we believe that both JP 1 and 2 agree with various other loads in warm and cold water, since the mean value of JP 1 noise and other sources noise is:

$$\frac{JP\ 1}{Other\ Thermal\ Sources} = 1.001 \pm 0.010$$

and the ratio of JP 1 and 2 is 0.997 with a standard deviation of 0.010.

TABLE 1

Noise Source Comparisons

Date of Measurement	Sources Compared	Ratio of Available Noise Power per °K
1968, July 10 to August 17	JP 1 compared to two 50 ohm sources at temperatures between 0° and 30 °C in water baths.	JP 1/Thermal Sources = 0.978 ± 0.005.
1969, December 23 to 1970, February 10	JP 1 compared to a 50 ohm source at water temperatures 0° - 11 °C.	JP 1/Thermal Sources = 1.026 ± 0.005.
1970, March 5 and 6 1970, June 22 and 23	JP 1 compared with A. Penzias standard thermal source in water bath 20 °C - 35 °C.	JP 1/A. Penzias Source = 1.002 ± 0.005.
1971, May 13 to June 19	JP 1 compared to two 50 ohm sources; one in ice, one at 25 °C.	JP 1/Thermal Sources = 0.996 ± 0.004.
1971, July 4 to 23	JP 1 compared with JP 2	JP 2/JP 1 = 0.997 ± 0.010.

3.3 The Efficiency of Power Transfer

The theory of the transfer of power is outlined in the Appendix. So long as both the noise source and the radiometer are well-matched, losses due to reflections are small. The VSWR's for JP 1 have been measured over the range 100 MHz to 2000 MHz and never exceed 1.08. JP 2 has been measured over the range 1.4 to 11.5 GHz (Figure 4). The radiometer used for the power comparisons reported here has an input VSWR of less than 1.1:1. The comparisons of noise power are therefore not affected (at the 1% level of accuracy) by mismatches. No evidence has been found that either JP 1 or JP 2 changes its VSWR appreciably when its temperature changes by 30 °K.

As Figure 4 shows, the VSWR of JP 2 is below 1.1:1 at frequencies up to 7 GHz, but that in the 7-11.5 GHz range the VSWR rises. Calibrations of radiometers whose input VSWR's are 1.1 or less will thus be good to about 1% up to 7 GHz. Above that frequency and in all cases where the input VSWR of the radiometer lies above about 1.2:1, quite important calibration errors can result due to imperfect power transfer. See the Appendix for further details and for ways of estimating the power transfer corrections in such cases.

3.4   The Speed of Response of the Source

The thermometer sensing the case temperature of the resistive element responds rapidly to demands for a temperature change. The speed of response of the noise power output has been measured for JP 2 and the results show that both for heating and cooling the noise power changes exponentially with time. Curves fitted to the heating and cooling portions show good fits with time constants for heating (T_1) and cooling (T_2) of

$$T_1 = 44 \text{ seconds} \qquad T_2 = 56 \text{ seconds} \tag{2}$$

There is no reason why these time constants should not differ—since they are determined by the ratios at which the heating/cooling device can exchange heat with the load and the surroundings.

To achieve a final state within 1% of the state at infinite time, 4.6 time constants are needed, so a good rule for JP 2 is to allow 5 minutes for both the heating and cooling stages.

3.5   Corrections to be Applied to JP 2

Suppose the temperature indicator on JP 2 is used between two indicated temperatures T_1 and T_2. Let the difference $T_1 - T_2 = \Delta T$. The difference in noise powers is not exactly ΔP where

$$\Delta P = kB\Delta T \tag{1}$$

because of the losses described in 4.1. A correction factor C must be calculated; it is less than unity and depends on the various losses and thus on frequency. Then the
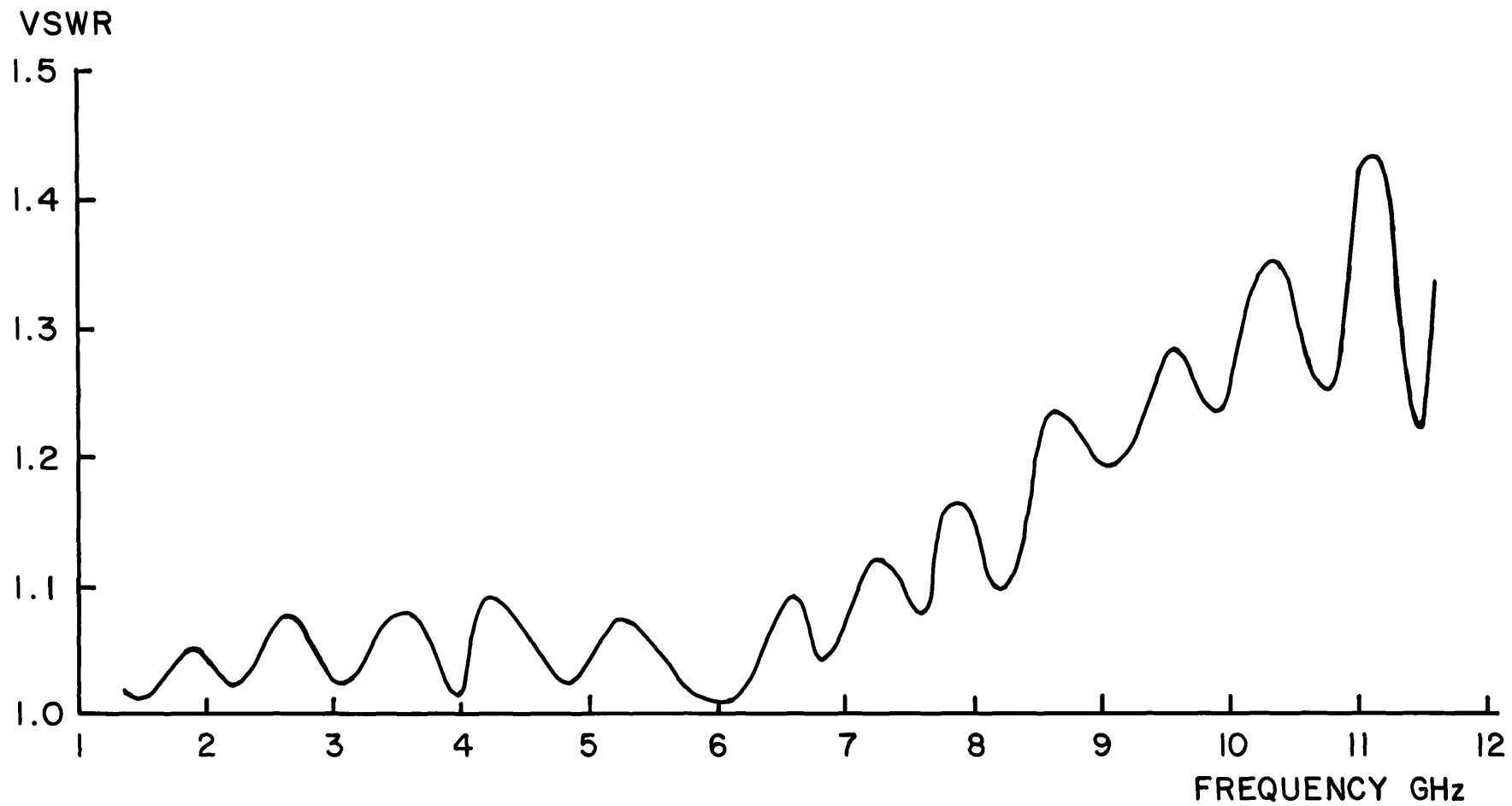
THE VSWR OF THE JP #2 CALIBRATOR

FIG. 4

difference in noise powers from the calibrator is C · ΔT.

The following losses contribute to C:

(a) Line and connector losses within JP 2.

(b) Losses in coaxial-to-waveguide transitions, if these are used.

In calculating the losses and their contribution to C, the results of measurements of line loss, connector loss and waveguide-to-coaxial transition loss were used. The measurements were made over the frequency range 1-11 GHz.

The value of C is then calculated, using where necessary the known line temperature conditions. The results are shown in Figure 5, where the correction factor is given for the use of the calibrator with and without a waveguide transition.

Increasing difficulty was experienced in measuring the small component losses as the measuring frequency increased above about 7 GHz. Therefore, although the correction factors of Figure 5 may be used with confidence up to that frequency, in the 7-11 GHz range there is more uncertainty in the value of these factors. This uncertainty, together with the higher VSWR above 7 GHz already described, suggests that errors of ± 5% may occur in measurements from 7-11 GHz made with this calibrator.

3.6   Some Rules for Using JP 2

(a) Allow of 1 hour warm-up time, so that the resistance sensor bridge may stabilize.

(b) Set approximate desired hot and cold temperatures on dials. Read ΔT from the display, not from the dials.

(c) When changing temperatures, allow 5 minutes warming or cooling times.*

---

* In warm rooms it may be desirable to blow air onto the calibrator head to improve heat exchange.
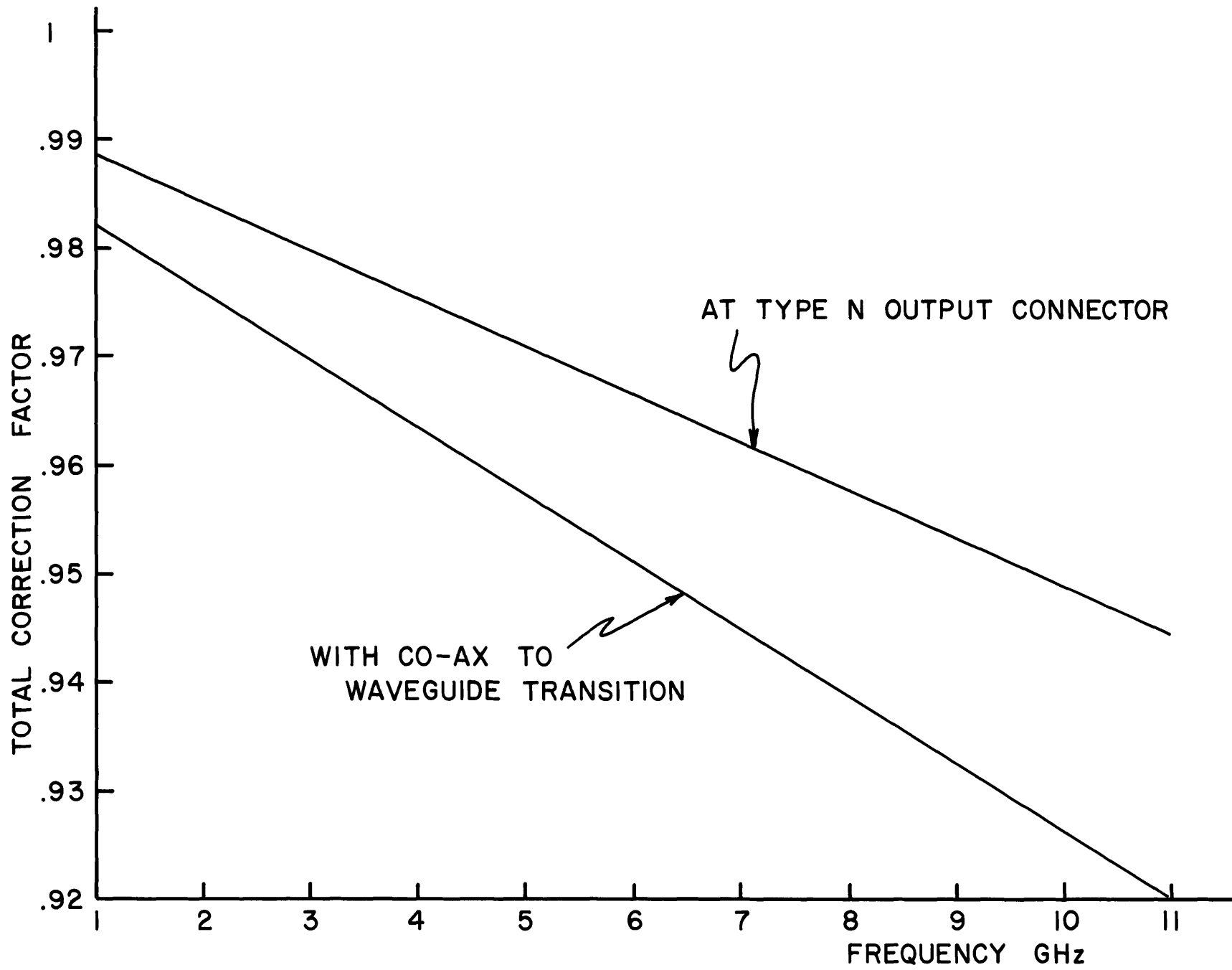
CORRECTION FACTOR TO BE APPLIED TO JP #2 AT FREQUENCIES
BETWEEN 1 & 11 GHz

FIG. 5

4.0   <u>References</u>

Stelzried, C. T. 1968, "Microwave Thermal Noise Standards," <u>IEEE Trans</u>.
<u>Microwave Th. and Tech.</u> <u>MTT-16</u>, 646-655.

Payne, John, "Thermal Calibration Unit," Electronics Division Internal
Report No. 63, September 1967.

APPENDIX

THE TRANSFER OF POWER BETWEEN AN IMPERFECTLY MATCHED GENERATOR AND AN IMPERFECTLY MATCHED LOAD

1. The Generator

The generator is a heated resistance, but it may include a reactive component which is not a noise generator. Any resistance R_g at absolute temperature $T°$ K is a source of a fluctuating e. m. f. given by

$$\overline{e_f^2} = 4kTR_g \, df \tag{1}$$

where $\overline{e_f^2}$ is the mean square voltage fluctuation at a frequency range df around f.

Thus, we may replace a noise generator by the equivalent circuit below where the generator resistance R_g and reactance X_g are to be considered noiseless and e_f is given by (1)
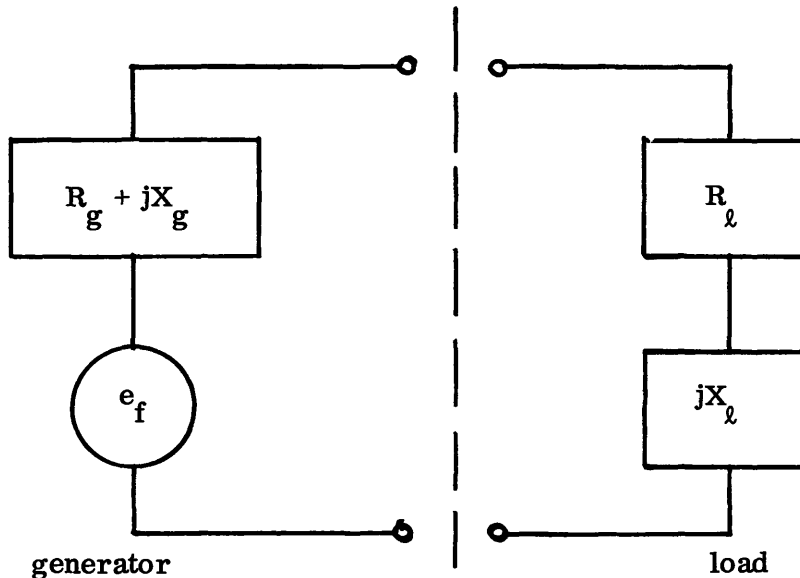

Figure A-1

The generator impedance is $Z_g = R_g + jX_g$.

2. The Load

Now consider the transfer of power from this generator to an arbitrary load with impedance $Z_\ell = R_\ell + jX_\ell$. We calculate the power delivered to the resistive component of the load.

The power delivered to R_ℓ is given by

$$P_\ell = |i|^2 R_\ell \qquad \text{where}$$

$$i = \frac{e_f}{Z_g + Z_\ell}$$

Thus, after a little algebra of complex numbers, we can see

$$|P_\ell| = \frac{e_f^2 R_\ell}{|Z_g + Z_\ell|^2} \tag{2}$$

Using (1), which gives the mean square value of e_f, we get the power delivered in a bandwidth B as

$$|P_\ell| = kTB \frac{4R_g R_\ell}{|Z_g + Z_\ell|^2} \tag{3}$$

3. Simple Cases

Equation (3) tells us all we need to know, but we will elaborate on it later. First note that the available power to the load is indeed kTB under two "matched" conditions.

(a) $R_g = R_\ell = R$, $X_g = X_\ell = 0$. This is the case of a purely resistive generator and load of equal value. $|Z_g + Z_\ell|^2$ becomes $(R_g + R_\ell)^2 = 4R^2$.

(b) $R_g = R_\ell = R$, $X_g = -X_\ell = 0$. This is the case of equal resistive components for generator and load and equal but opposite reactive components (one is inductive and one is capacitative).

Now $\left| Z_g + Z_\ell \right|^2 = \left| (R_g + R_\ell) + j(X_g + X_\ell) \right|^2 = 4R^2$ as before. From now on we will consider only the factor

$$\eta = \frac{4 R_g R_\ell}{\left| Z_g + Z_\ell \right|^2} \tag{4}$$

as a measure of the efficiency of power transfer. When $n = 1$ power transfer is perfect, when $n < 1$, some power $(1 - n)$ does not reach the load.

4. A Real Case

In the present note we are concerned with the value of η when the generator is, for example, JP 2, and the load is the measuring radiometer. To determine η we can measure Z_g and Z_ℓ and apply (4). The measurements were made over a range of frequencies covering the radiometer bandpass (B) and the points of measurement were the output type N connector of JP 2 and the input type N connector leading to the radiometer. The results are shown as admittance plots in Figure A-2. As an example, we take the values of Z_g and Z_ℓ corresponding to 1410 MHz. (For very precise work or where Z_g or Z_ℓ varies widely over B we should calculate η over B and take a mean value).

From the admittance plots we get

$$\left. \begin{array}{l} 1/Z_g = 20.5 + 1.2j \text{ millimhos} \\ 1/Z_\ell = 22.0 - 1.0j \text{ millimhos} \end{array} \right\} \tag{5}$$

Hence

$$\left. \begin{array}{l} Z_g = 48.6 - 2.85j \text{ ohms} \\ Z_\ell = 45.4 + 2.06j \text{ ohms} \end{array} \right\} \tag{6}$$

and we find η by

$$\eta = \frac{4 \times 48.6 \times 45.4}{(48.6 + 45.4)^2 + (2.06 - 2.85)^2}$$
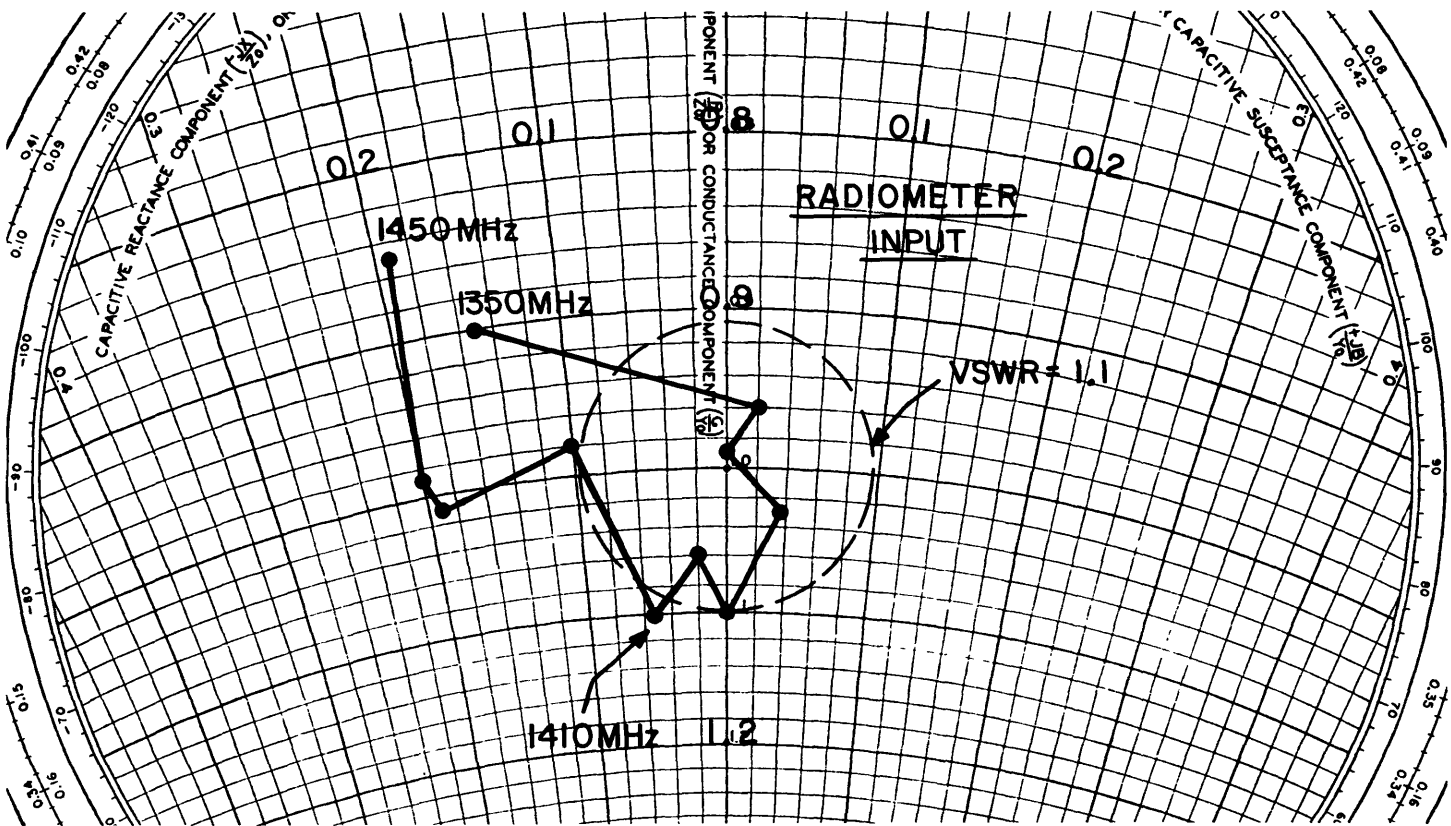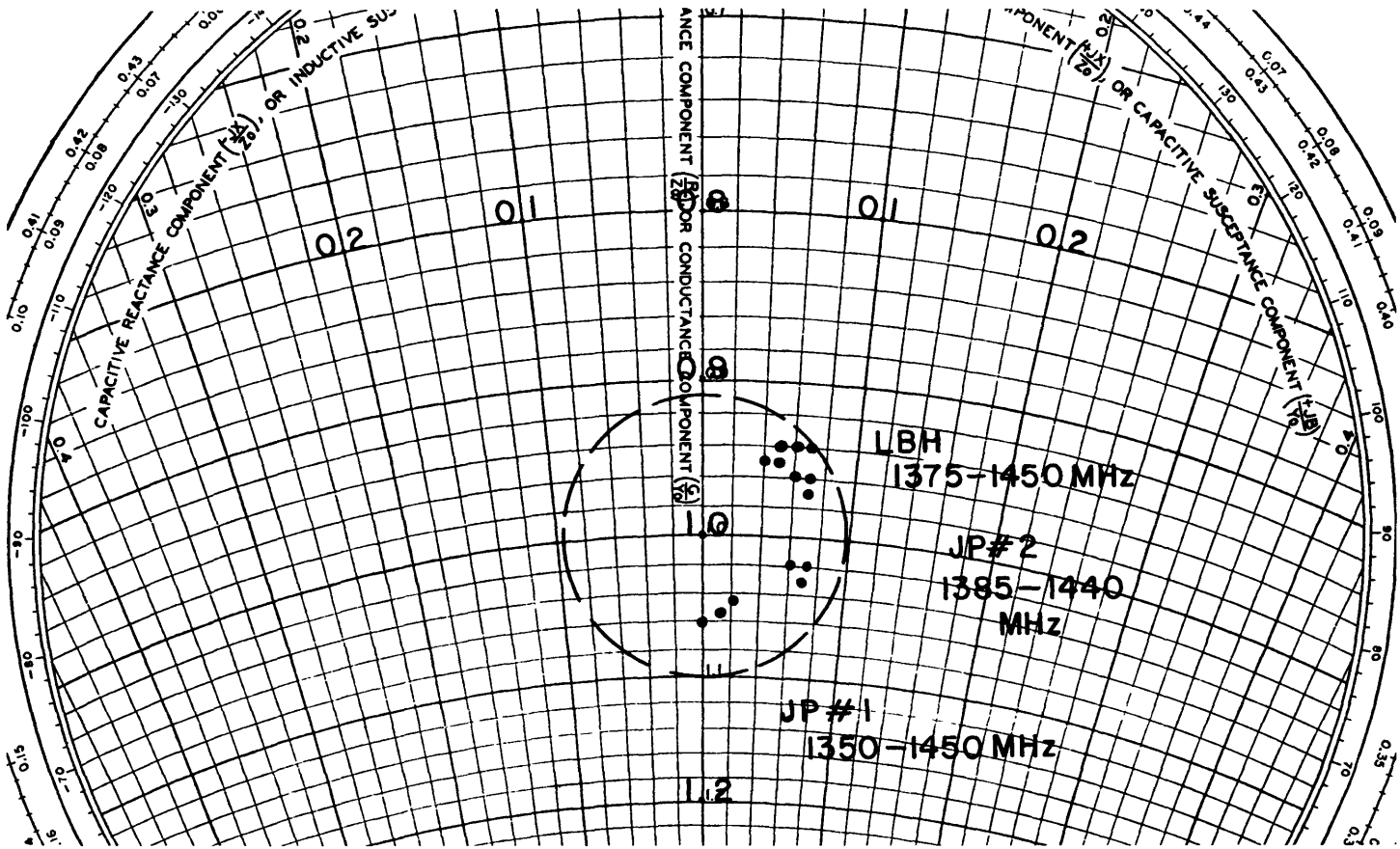
$$\eta = 0.9988 \tag{7}$$

Figure A-2   Admittance Plot for the Sources JP 1, JP 2, LBH and the Radiometer

Input (Y_0 = 20 millimhos)

Similar calculations lead to the following values for η

Transfer Condition	Frequency	η
JP 1 to R_x	1410 MHz	0.9992
JP 2 to R_x	1410 MHz	0.9988
LBH to R_x	1410 MHz	0.9980

The very close equality of the values of η show that negligible experimental errors due to imperfect power transfer arise in the JP 1 − JP 2 comparisons and in the observations with the Calibration Horn.

5. Some Further Useful Relationships

Although Equation (4) combined with measurements of Z_g and Z_ℓ can be used to derive η, it is much more usual to have only measurements of the voltage standing wave ratios of the generator and the load measured on a lossless line of characteristic impedance Z_0. As we shall see, this information cannot be used to determine η, but can be used to set limits within which η must lie. In general noise calibrations, such limits are useful. Also, we have not specifically dealt with the case where a variable line length joins generator and load. To discuss these cases, Equation (4) is more useful in a different form.

For help in what follows, consult any good text on transmission lines (Electromagnetic Energy Transmission and Radiation; Adler, Chu and Fano, Wiley and Sons, 1960, is an example).

Instead of dealing with the impedance discontinuities placed on a lossless* transmission line we use the concept of the reflection coefficient at any point on a line. This is a complex quantity, and is defined by

$$\Gamma(x) = \frac{V_-(x)}{V_+(x)} \tag{8}$$

where at x on the line a discontinuity has produced from a forward travelling voltage wave $V_+(x)$ a reflected voltage wave $V_-(x)$.

If the reflection is caused by an impedance Z_ℓ terminating a line (Z_0), it is easy to show

$$\Gamma_\ell = \frac{Z_\ell - Z_0}{Z_\ell + Z_0}$$

or, using normalized impedances $Z_{n\ell} = \frac{Z_\ell}{Z_0}$

$$\Gamma_\ell = \frac{Z_{n\ell} - 1}{Z_{n\ell} + 1} \tag{9a}$$

and the equivalent expression

$$Z_{n\ell} = \frac{1 + \Gamma_\ell}{1 - \Gamma_\ell} \tag{9b}$$

---

* For the power transfer discussion, the assumption of lossless lines is satisfactory. However, in practice, cases may arise when the line loss and the noise power developed by the line need to be considered.

We can now rewrite Equation (4) in terms of

$$\Gamma_g = \frac{Z_{ng} - 1}{Z_{ng} + 1} \quad \text{and} \quad \Gamma_\ell = \frac{Z_{n\ell} - 1}{Z_{n\ell} + 1}$$

as follows:

$$\eta = \frac{(1 - |\Gamma_g|^2)(1 - |\Gamma_\ell|^2)}{|1 - \Gamma_g \Gamma_\ell|^2} \tag{10}$$

The steps from (4) to (10) require a fairly straightforward application of complex number algebra.

a. Load, Generator and Line

Now consider the case shown in Figure A-3 when the generator sends power to the load via a lossless line.

Our expression (10) still describes the power delivered across the x = ⁻d plane if we use for the reflection coefficient the value appropriate to that plane. But, in terms of Γ_ℓ, it is easy to write a value for Γ_d, the reflection coefficient at x = ⁻d. The expression is derived in a way similar to that which derives the input impedance to the line length d terminated by Z_ℓ, (and can in fact be got from a Smith chart in practical cases). We find that

$$\Gamma_d = \Gamma_\ell \, e^{2j\beta\ell} \tag{11}$$

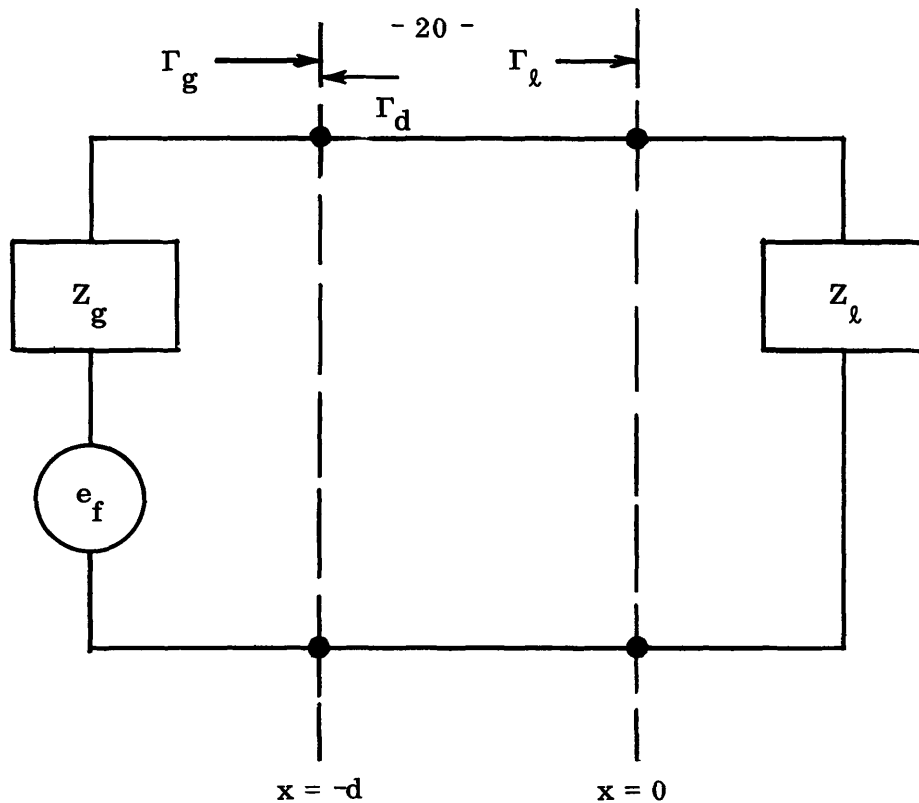where $\beta = 2\pi/\lambda$ (λ is the wavelength on the line).

$\Gamma_g \longrightarrow$ $\Gamma_\ell \longrightarrow$

Γ_d

Z_g Z_ℓ

e_f

x = -d   x = 0

Figure A-3

Note also to substitute in (10) that:

$$\left|\Gamma_d\right| = \left|\Gamma_\ell \ e^{2j\beta\ell}\right| = \left|\Gamma_\ell\right| \tag{12}$$

Hence, our expression for η in (10) becomes

$$\eta = \frac{(1 - \left|\Gamma_g\right|^2)(1 - \left|\Gamma_\ell\right|^2)}{\left|1 - \Gamma_g \Gamma_\ell \ e^{2j\beta\ell}\right|^2} \tag{13}$$

where, because of (12), we were able to substitute $\left|\Gamma_\ell\right|$ for $\left|\Gamma_d\right|$ in the top line and the $e^{2j\beta\ell}$ factor only occurs in the denominator.

b. **Maximum and Minimum Values for η**

Equation (13) has a practical value although it is cumbersome to use except numerical cases. It gives limits to the values, for given Γ_g and Γ_ℓ 's, that η can have. We can see this by noting that the denominator of (13) is of the form:

$$\left|1 - \left|\Gamma_g\right| \left|\Gamma_\ell\right| \ e^{j\phi}\right|^2$$

where we have incorporated all the phase angles together into ϕ. Thus the denominator becomes:

$$1 - 2 \left|\Gamma_g\right| \left|\Gamma_\ell\right| \quad \cos \phi + \left|\Gamma_g\right|^2 \left|\Gamma_\ell\right|^2$$

Hence it assumes maximum and minimum values of $(1 \pm \left|\Gamma_g\right| \left|\Gamma_\ell\right|)^2$, and in turn the maximum and minimum values for η are

$$\left.\begin{array}{l} \eta_{max} = \dfrac{(1 - \left|\Gamma_g\right|^2)\ (1 - \left|\Gamma_\ell\right|^2)}{(1 - \left|\Gamma_g\right| \left|\Gamma_\ell\right|)^2} \\[4mm] \eta_{min} = \dfrac{(1 - \left|\Gamma_g\right|^2)\ (1 - \left|\Gamma_\ell\right|^2)}{(1 + \left|\Gamma_g\right| \left|\Gamma_\ell\right|)^2} \end{array}\right\} \tag{14}$$

The expressions (14) are the basis for a useful rule for calculating maximum and minimum losses. This rule is derived as follows:

Assume the mismatch losses are due to reflection and can be described by a VSWR. Then the VSWR's associated with the losses (14) would be

$$1 - \eta_{min} = \left(\frac{(VSWR)_{max} - 1}{(VSWR)_{max} + 1}\right)^2$$

$$1 - \eta_{max} = \left(\frac{(VSWR)_{min} - 1}{(VSWR)_{min} + 1}\right)^2$$

We thus derive the following expressions for the VSWR's which, if they existed, would cause power reflections $(1 - \eta_{min})$ and $(1 - \eta_{max})$. Note that $(1 - \eta_{min})$ is the larger power reflected.

$$(VSWR)_{min} = \frac{1 + |\Gamma_g|}{1 - |\Gamma_g|} \cdot \frac{1 - |\Gamma_\ell|}{1 + |\Gamma_\ell|} = \frac{(VSWR)_g}{(VSWR)_\ell} \left.\rule{0pt}{40pt}\right\} \tag{15}$$

$$(VSWR)_{max} = \frac{1 + |\Gamma_g|}{1 - |\Gamma_g|} \cdot \frac{1 + |\Gamma_\ell|}{1 - |\Gamma_\ell|} = (VSWR)_g \times (VSWR)_\ell$$

The meanings of $(VSWR)_g$ and $(VSWR)_\ell$ are that these are the VSWR's of the generator and load respectivity when used separately to terminate a Z_0 line.

Hence, we derive the rule:

To calculate the maximum and minimum losses due to mismatches in a system as shown in Figure A-3, first determine the VSWR's of load and generator separately. Call them $(VSWR)_g$ and $(VSWR)_\ell$. Choose the greater (suppose it is $(VSWR)_\ell$. Then the maximum reflected power possible is calculated by

$$\left\{ \frac{(VSWR)_{max} - 1}{(VSWR)_{max} + 1} \right\}^2$$

with $(VSWR)_{max} = (VSWR)_g \times (VSWR)_\ell$ $\qquad (16)$

And the minimum reflected power possible is calculated by

$$\left\{ \frac{(VSWR)_{min} - 1}{(VSWR)_{min} + 1} \right\}^2$$

with $(VSWR)_{min} = \frac{(VSWR)_\ell}{(VSWR)_g}$ $\qquad (17)$

(Note: In (17) the larger VSWR is in the numerator.)

c. **A Numerical Example**

Suppose the generator has a VSWR of 1.1 and the load a VSWR of 1.2.

$1.2/1.1 = 1.091$, $1.2 \times 1.1 = 1.32$.

$$\text{Max reflection loss} = \left(\frac{1.32 - 1}{1.32 + 1}\right)^2 = 1.9\%$$

$$\text{Min reflection loss} = \left(\frac{1.091 - 1}{1.091 + 1}\right)^2 = 0.19\%$$

d. **Plots of Maximum and Minimum Loss**

Plots have been published which are based on (16) and (17), see Figure A-4 for example.

e. **Effect of Varying Line Length**

As the length of line joining generator and load in Figure A-3 is altered, η must alter in a periodic fashion between the maximum and minimum values of Equation (14). A complete cycle of variation is included when the line length alters by half a line wavelength. A plot of such a variation in η is shown in Figure A-5 calculated for the case of JP 2 and the radiometer as a load. The maximum and minimum values of η were

$$\eta_{max} = .9994$$

$$\eta_{min} = .9926$$

POWER LOSS CURVES

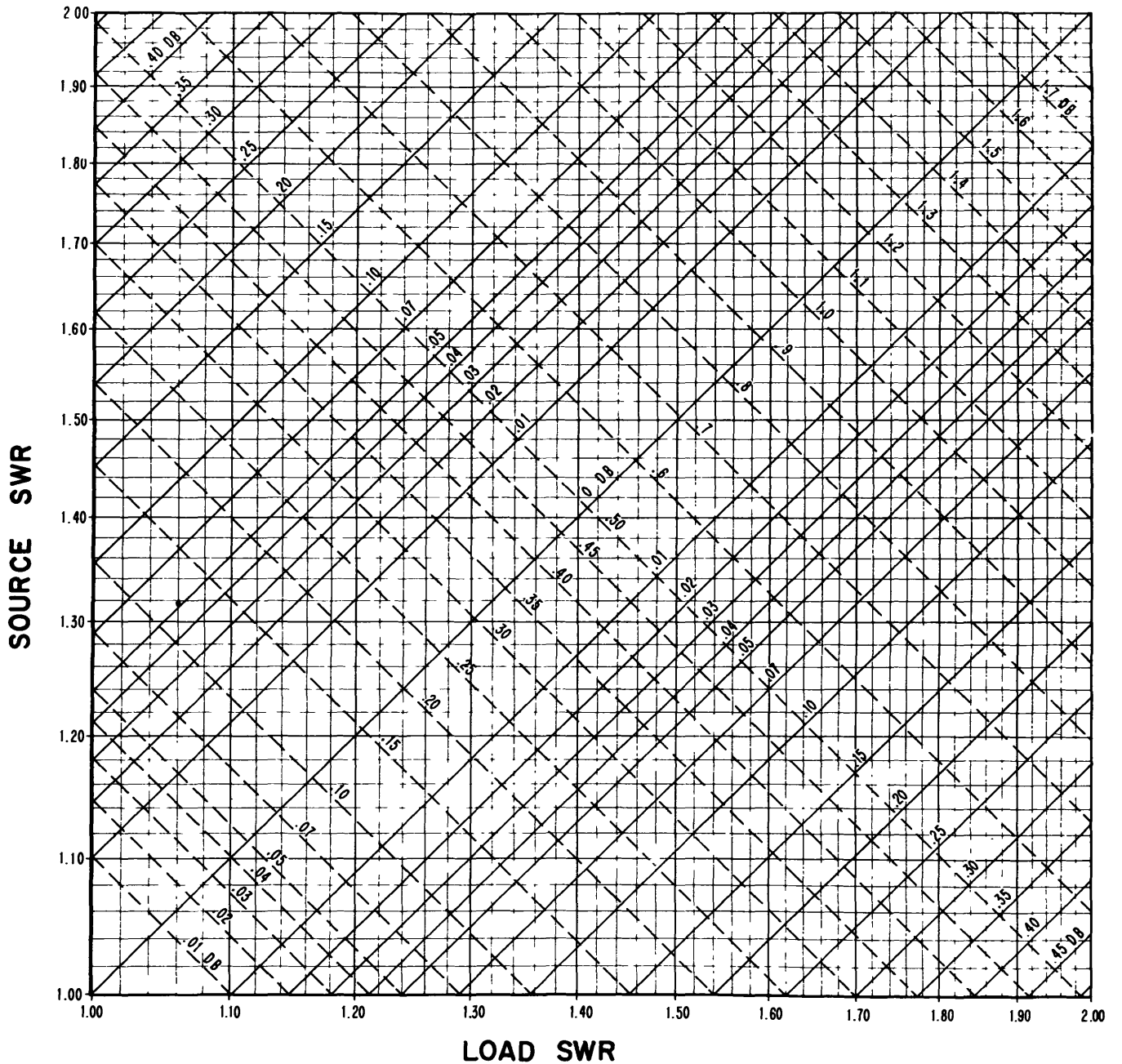## (SOLID LINES INDICATE MINIMUM POWER LOSS, BROKEN LINES MAXIMUM POWER LOSS)

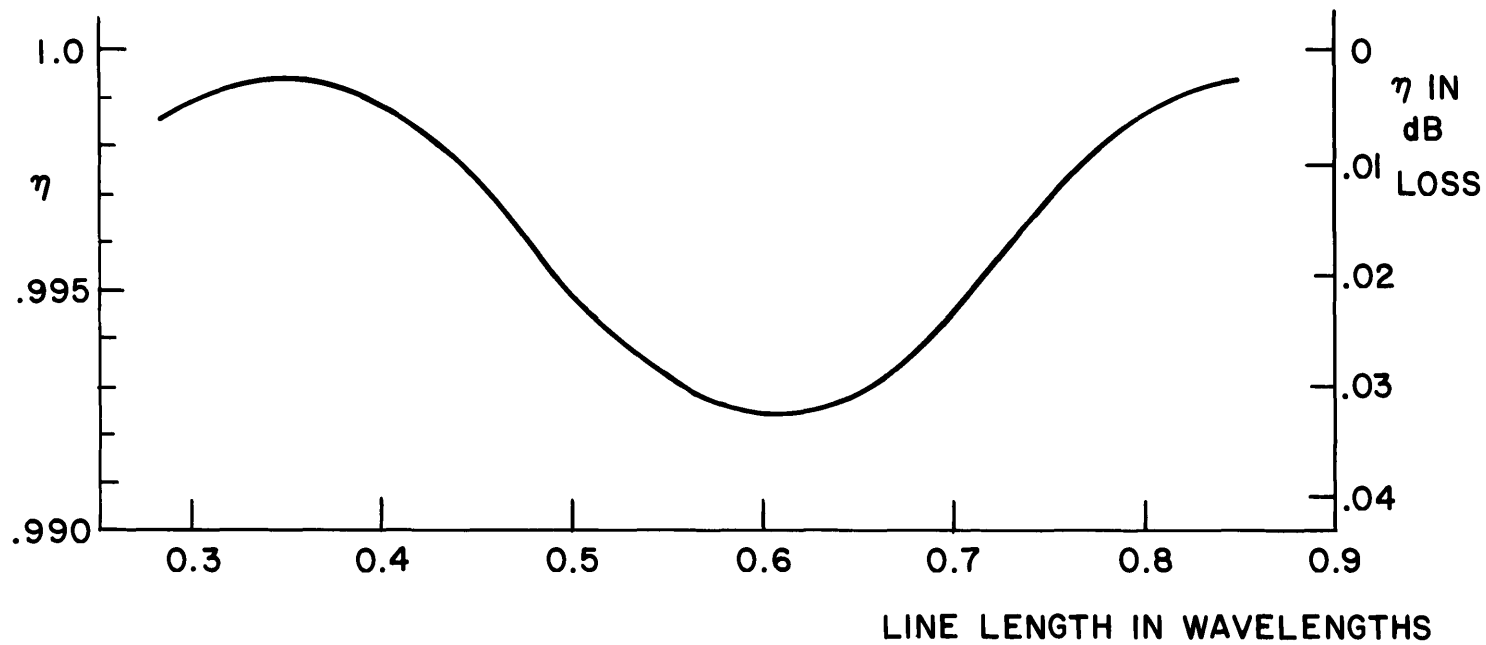**LOAD SWR**

(y-axis label) **SOURCE SWR**

Figure A-4

FIG. A—5

Calculated Transmission Efficiency η for a Lossless Line of Varying Length

Generator is (48.85 - 2.87 j) ohms

Load   is (45.36 + 2.06 j) ohms